Journal of Robotics and Control (JRC)
Volume 4, Issue 5, 2023
ISSN: 2715-5072, DOI: 10.18196/ jrc.v4i5.19588

Design and Develop a Non-Invasive Pulmonary Vibration Device for Secretion Drainage in Pediatric Patients with Pneumonia

Anantasak Wongkamhang [1], Nathamon Wuttipan [2], Rawiphon Chotikunnan [3*], Kittipan Roongprasert [4], Phichitphon Chotikunnan [5], Nuntachai Thongpance [6], Manas Sangworasil [7], Anuchart Srisiriwat [8]
[1, 3, 4, 5, 6, 7] College of Biomedical Engineering, Rangsit University, Pathum Thani, Thailand
[2] School of Nursing, Mae Fah Luang University, Chiang Rai, Thailand
[8] Department of Electrical Engineering, Pathumwan Institute of Technology, Bangkok, Thailand
Email: [1] anantasak.w@rsu.ac.th, [2] nathamon.sri@mfu.ac.th, [3] rawiphon.c@rsu.ac.th, [4] kittipan.r@rsu.ac.th, [5] phichitphon.c@rsu.ac.th, [6] nuntachai.t@rsu.ac.th, [7] manas.s@rsu.ac.th, [8] anuchart@pit.ac.th
*Corresponding Author

***Abstract*—The study aimed to develop a non-invasive pulmonary vibration device, specifically tailored for pediatric patients, to address a range of pulmonary conditions. The device employs a PID control system to ensure consistent and precise vibrations. The primary contribution of this research is the successful development, testing, and implementation of this innovative device. Utilizing technical components such as an Arduino, a vibration DC motor, and an ADXL335 accelerometer, the device was engineered to deliver stable and continuous vibrations even when subjected to external pressures or interactions with the patient. Controllers, including P, PI, PD, and PID types, were rigorously compared. The Ziegler-Nichols tuning technique was applied for meticulous evaluation of vibration control specifically within the context of this non-invasive pulmonary vibration device. Our findings revealed that the PID controller displayed superior accuracy in vibration control compared to P, PI, and PD controllers. Clinical trials involving pediatric patients showed that the PID-controlled device achieved treatment outcomes comparable to conventional methods. The device's precise control of vibration strength provides an added benefit, making it a well-tolerated, non-invasive treatment option for various pulmonary conditions in pediatric patients. Future research is necessary to assess the long-term effectiveness of the device and to facilitate its integration into standard clinical practice. In summary, this study represents a significant advancement in pediatric pulmonary care, demonstrating the critical role that PID control systems adapted for non-invasive pulmonary vibration devices can play in enhancing treatment precision and outcomes.**

Keywords—Pulmonary; PID Control; Vibration Device; Pneumonia.

I. INTRODUCTION

Pneumonia remains a substantial concern in pediatric care, accounting for a high rate of hospitalizations and fatalities, especially among children under the age of five [1]-[5]. In Thailand, the morbidity rate for pediatric pneumonia in the age group of 0-4 years is alarmingly high, estimated at 1,975.97 cases per 100,000 population [2], [6]. Acknowledging the gravity of the situation, the Ministry of Public Health in Thailand has reported that up to 50 percent of children under 5 are affected by pneumonia, with life-threatening severe cases comprising 7-13 percent of instances [7]. Traditionally, viruses have been pinpointed as the primary causative agents of pneumonia in children, influencing the respiratory tract and resulting in symptoms like shortness of breath and respiratory failure [2]-[10]. Among the range of available treatments, chest physical therapy stands out as an essential component of effective pediatric pneumonia management [1], [5], [8]-[13]. However, traditional techniques such as percussion and lung vibration come with limitations and are not effective across all cases. The success of these methods largely depends on the expertise of the healthcare provider [11]-[13]. Moreover, devices engineered to enhance sputum drainage, like chest vibrators, are typically only accessible in well-funded healthcare settings due to their elevated costs [10], [14]-[16].

To address these shortcomings, this study aims to introduce an innovative and cost-effective pulmonary vibration device based on Arduino technology, which has shown a wide range of applicability across various system control fields [17]-[43]. Notably, the technology also demonstrates applicability in motor control systems [44]-[52]. The device features a Vibration DC motor and an ADXL335 and is managed by a Proportional-Integral-Derivative (PID) control system. PID control systems are well regarded for their user-friendly design and effectiveness in maintaining system stability. Various methods for system optimization, such as the Ziegler and Nichols technique, have been examined [53]-[74].

The primary objective of this research is to assess the effectiveness of this Arduino-based, non-invasive pulmonary vibration device within the framework of pediatric pneumonia care. This study employs Donabedian's Conceptual Outcome Theory to evaluate the quality of nursing care and utilizes Cohen's table for one-tailed hypothesis testing on the total sample [75], [76]. In summary, the study delves into the development, implementation, and evaluation of this non-invasive pulmonary vibration device. It outlines its promising results in both controlled experimental settings and real-world case studies. These findings are anticipated to align with existing therapeutic interventions and will contribute to our broader understanding of effective treatments for pneumonia [77]-[85].

II. RESEARCH METHOD

A. System Design and Components

The pulmonary vibration device is designed to improve lung function and is composed of two principal components, as depicted in Fig. 1 and Fig. 2. At the core of the system is the controller box, which contains an Arduino Uno board, a variable resistor, a button switch, an LCD screen, and a motor driver. This controller box processes the incoming data and controls the vibrational force applied. In addition to the controller box, the second major component is the vibration device. This unit utilizes a DC12V motor, which is fitted with a cam and an accelerometer to monitor its operational dynamics. The system provides real-time feedback through an LCD screen. Safety measures, including an emergency stop button and software set limitations on vibration intensity, are incorporated into the design, with all safety protocols receiving approval under IRB document COA: 009/2021 and Protocol No: EC 20107-19.

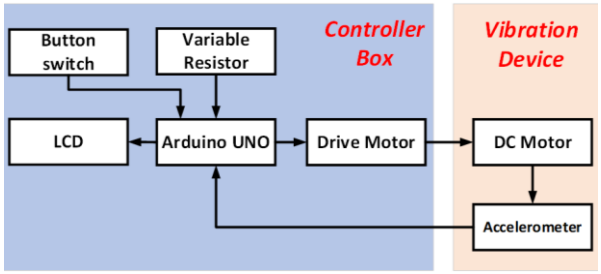

Fig. 1. Block diagram of the overall system

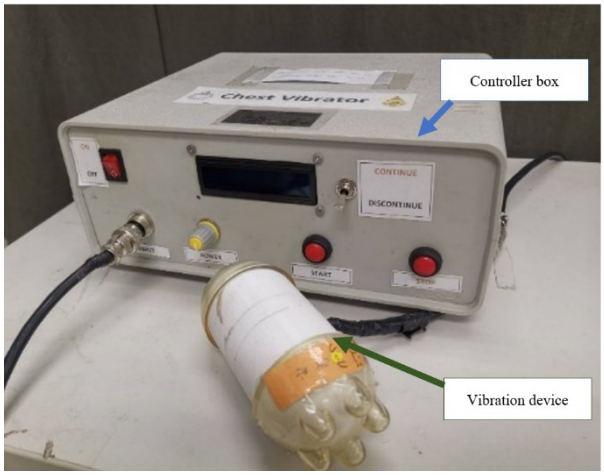

Fig. 2. Non-invasive pulmonary vibration device

The operation of the device follows a flowchart shown in Fig. 3, where users initially adjust the variable resistor to set their desired vibration force. Users can choose between two modes of operation, continuous and intermittent. In the intermittent mode, the device vibrates for a span of 10 seconds followed by a 5-second pause, and this cycle continues until the user manually stops the operation. The vibration apparatus and vibration device used in this research are shown in Fig. 4 and Fig. 5.

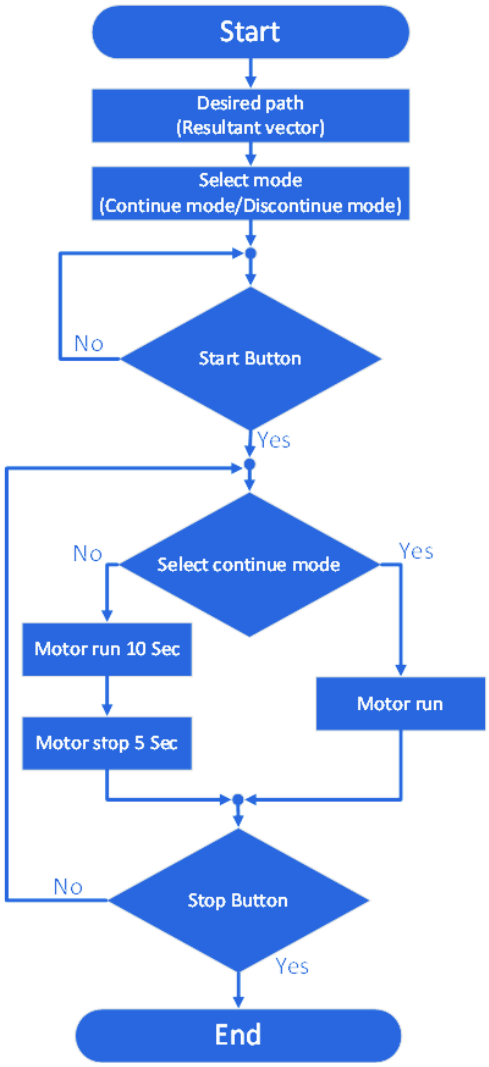

Fig. 3. Program flowchart of pulmonary vibration device

Fig. 4. Vibration apparatus (controller box)

Fig. 5. Vibration device

B. Hardware Components and Implementation

This section explains the components that had been used including Arduino Uno, ADXL335, vibration DC motor, DC motor drivers, and variable resistor.

The Arduino Uno serves as the system's main microcontroller and is featured in Fig. 6. Built around the ATmega328P microcontroller chip, it offers versatile control over a wide variety of channels. The board comes equipped with 14 digital I/O pins and six analog input pins, all operating on a 5V power supply.

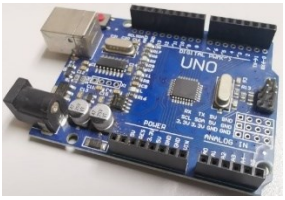

Fig. 6. Arduino Uno

The ADXL335 accelerometer, highlighted in Fig. 7, is specifically engineered to measure acceleration in three dimensions X, Y, and Z. The sensor is not only compatible with the Arduino Uno but also exhibits high accuracy with sensitivity ranges spanning from 270 to 330mV/g. It has the ability to accurately measure and represent acceleration within a range of ±3g.

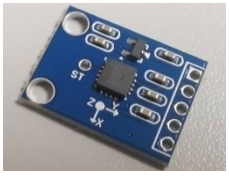

Fig. 7. ADXL335

Featured in Fig. 8, the DC12V vibration motor is central to the device's functioning. Its key specifications include a high operational speed of 4150 revolutions per minute and a load current of 0.1A, making it highly efficient in generating tactile feedback.

Fig. 8. Vibration DC motor

The L298N motor driver is seen in Fig. 9 and is designed to control two motors independently. It accepts an input voltage that can range from 7V to 35V and can drive motors that require a current of up to 2A.

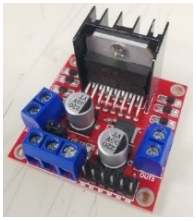

Fig. 9. DC motor driver

Lastly, the variable resistor is depicted in Fig. 10. It plays a crucial role by allowing users to manually adjust the vibration force. This level of customization is crucial for tailoring the device's operation to meet individual user needs.

Fig. 10. Variable resistor

III. NORMALIZATION OF ACCELEROMETER

The design of the accelerometer normalization in this study aims to estimate the resulting vector of the accelerometer caused by vibration, which can be utilized to control the PID controller system. Since the direct use of accelerometer signal values to control the vibration function is not efficient, normalization of the accelerometer signals is necessary. This allows for more effective control of the vibration function and can lead to improved performance of the system.

The program flowchart design for normalization is displayed in Fig. 11. The design starts by receiving signal values from the accelerometer, specifically from the X, Y, and Z axes, which are represented by equations (1), (2), and (3). The received signal values are then converted into vector results, as shown in the last equation (16). Afterward, the resultant vector of g is calculated using an average filter, as seen in equation (17). This process is crucial for accurately estimating the resulting vector of the accelerometer, which is used to effectively control the vibration function in the PID controller system.

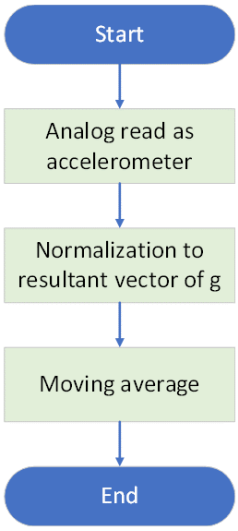

Fig. 11. Program flowchart of normalization

The ADXL335 sensor receives an analog signal from the accelerometer, which provides the signal value for the X, Y, and Z axes. These values can be represented mathematically as equations (1), (2), and (3).

$$a_x(k) = input\ analog\ x(k) \quad (1)$$

$$a_y(k) = input\ analog\ y(k) \quad (2)$$

$$a_z(k) = input\ analog\ z(k) \quad (3)$$

After receiving the analog signals from the ADXL335 sensor in the x, y, and z axes, the program determines the maximum and minimum values of the readings and stores them within a range of N_i, which is set to 10 in this study. This process is demonstrated by equations (4), (6), and (8), which represent the maximum values on the x, y, and z-axes, and equations (5), (7), and (9), which represent the minimum values on the x, y, and z-axes. The variable k represents the time interval at the present moment.

$$y_{x\_max}(k) = \max_{(k-N_i)\to k}[a_x(k-N_i) \quad \cdots \quad a_x(k)] \quad (4)$$

$$y_{x\_min}(k) = \min_{(k-N_i)\to k}[a_x(k-N_i) \quad \cdots \quad a_x(k)] \quad (5)$$

$$y_{y\_max}(k) = \max_{(k-N_i)\to k}[a_y(k-N_i) \quad \cdots \quad a_y(k)] \quad (6)$$

$$y_{y\_min}(k) = \min_{(k-N_i)\to k}[a_y(k-N_i) \quad \cdots \quad a_y(k)] \quad (7)$$

$$y_{z\_max}(k) = \max_{(k-N_i)\to k}[a_z(k-N_i) \quad \cdots \quad a_z(k)] \quad (8)$$

$$y_{z\_min}(k) = \min_{(k-N_i)\to k}[a_z(k-N_i) \quad \cdots \quad a_z(k)] \quad (9)$$

The process of determining the offset value of the ADXL335 sensor typically involves setting it to a value of 1.65V and then converting the signal back to an analog signal. However, if this value is used, it will not be possible to control the vibration function effectively as the vibration device of grip angle can affect the measurement.

This study involved designing the offset value of the ADXL335 sensor in order to account for the varying angles and coordinates at which the vibration device may be caught or shaken. This was achieved through the use of equations (10), (11), and (12), which were used to determine the offset values for the x, y, and z axes, respectively.

$$zero_{g_x} = \left(\frac{y_{x\_max}(k) + y_{x\_min}(k)}{2}\right) \quad (10)$$

$$zero_{g_y} = \left(\frac{y_{y\_max}(k) + y_{y\_min}(k)}{2}\right) \quad (11)$$

$$zero_{g_z} = \left(\frac{y_{z\_max}(k) + y_{z\_min}(k)}{2}\right) \quad (12)$$

Once the offset value of the ADXL335 sensor has been determined, the gravitational values (g) in the x, y, and z axes can be calculated using equations (13), (14), and (15), respectively. The scale_factor used in the equations is the sensitivity factor at u^X, u^Y, u^Z, which has been set to 112.33.

$$u^X(k) = \frac{a_x(k) - zero_{g_x}}{scale\_factor} \quad (13)$$

$$u^Y(k) = \frac{a_y(k) - zero_{g_y}}{scale\_factor} \quad (14)$$

$$u^Z(k) = \frac{a_z(k) - zero_{g_z}}{scale\_factor} \quad (15)$$

The resultant vector of gravitational values, known as g_{sum}, is a measure of the total gravitational force acting on the system. It is calculated using equation (16).

$$g_{sum}(k) = \sqrt{u^X(k)^2 + u^Y(k)^2 + u^Z(k)^2} \quad (16)$$

To determine the resultant vector of gravitational values (g) using an average filter, a moving average or average filter method is applied. This statistical method analyzes data by creating a series of averages from different subsets of the full dataset. The average filter method helps to identify trends and patterns in the data while smoothing fluctuations or noise. This method is often used in time series analysis to help identify trends and make predictions about data points. In this research, the resultant vector of g is calculated using an average filter, which is represented by equation (17).

$$g_{avg}(k) = \frac{1}{N_y}\sum_{k-N_y}^{k} g_{sum} \quad (17)$$

Equation (17) represents the moving average filter used to calculate the average of a specified number of data points at each step time. The output of the filter, denoted by g_{avg}, is calculated from the input gravitational data, denoted by g_{sum}, with N_y representing the number of data points used to calculate the average and k representing the step time. In this study, the input data consisted of 20 data points with a sampling time of 10 ms.

IV. PID CONTROLLER DESIGN

This study focuses on the design of a PID control system for a pulmonary vibration device using a vibration DC motor. The output value of the system is represented by g_{avg} or $y(k)$, while the vibration error is represented by $e(k)$, which can be calculated using equation (18).

$$e(k) = y_d(k) - y(k) \quad (18)$$

The control law of PID generating the feedforward control signal is given by (19).

$$u_j(k) = K_p e_j(k) + K_i T_s \sum_{v=0}^{k} e_j(v) + \frac{K_d N}{1 + NT_s}\left(\frac{e_j(k) - e_j(k-1)}{T_s}\right) \quad (19)$$

In control systems, a PID controller is a feedback control mechanism used to maintain a process variable at a desired setpoint. The controller is made up of three parameters: proportional gain (K_p), integral gain (K_i), and derivative gain (K_d), which are used to calculate the control signal u_j that is applied to the system. A derivative filter parameter N is also included to reduce noise amplification in the system, and in this research, N has been assigned a value of 100. The sampling time T_s is the duration between successive calculations of the control signal, and for this study, the value of T_s is 0.01 seconds. The PID controller's fundamental structure is demonstrated in Fig. 12, where the error signal $e_j(k)$ is the difference between the desired setpoint and the process variable. The controller output is obtained by summing the contributions from the proportional, integral, and derivative control actions.

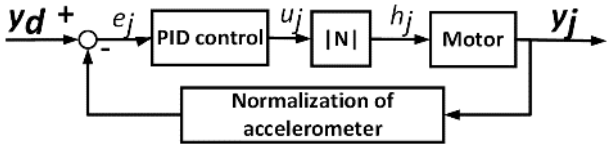

Fig. 12. Block diagram of the PID controller

The vibration device system is managed by a PID controller that is initially tuned using the Ziegler-Nichols method, followed by manual tuning to further optimize the system's performance. Table I shows the gain values of the PID system for each axis, which are used for controlling the vibration device system.

TABLE I. PID GAIN VALUES OF JOINT R

Joint	K_p	K_i	K_d
P controller	165	-	-
PI controller	125	35	-
PD controller	130	-	25
PID controller	120	30	15

The signal value, y_d, depicted in Fig. 12, is obtained from the variable resistor. In this study, the value of y_d can be determined using equation (20), where the value of g_{max} is set to 1.2.

$$y_d(k) = \frac{input\ analog\ variable\ resistor(k)\ \times g_{max}}{1023} \quad (20)$$

Based on the results shown in Fig. 12, the $|N|$ value in the control box is obtained after the control input signal of the PID system. The purpose of normalization is to ensure that the control input value is within the range of 0 to 255, which is necessary for PID control of the system. The normalization is carried out according to equation (21), which imposes certain conditions on the control input value.

$$h_j(k) = \begin{cases} u_j(k) > 255\,, u_j(k) = 255 \\ u_j(k) < 255\,, u_j(k) = u_j(k) \\ u_j(k) < 0\,, u_j(k) = 0 \end{cases} \quad (21)$$

V. EXPERIMENTAL RESULT

This section presents four sets of experimental results. Firstly, the vibrating head system undergoes testing to ascertain its frequency within the range of 0 to 20 Hz. Secondly, an analysis of the efficiency of the PID controller, along with the design of P, PI, PD, and PID controllers, is conducted to determine which controller exhibits the highest level of system control efficiency. The third part involves an evaluation of actual trials involving pediatric patients, comparing the results to conventional treatment methods where manual massage is used to dissolve mucus in the lungs. Lastly, it involves summarizing the overall experimental findings and their interconnections. The detailed outcomes of these experiments are provided as follows.

A. First Result

In the first set of results, a PID controller was used to vibrate continuously for 30 seconds, followed by measuring the signal frequency using the pseudospectrum method. The main goal was to evaluate the performance of the vibration device and determine if the signal being tested was within the range of 0-20 Hz. The results indicated that the vibration device had a frequency range lower than 1 with very high power/frequency. Additionally, a range of 4 Hz and 10 Hz had a medium power/frequency, while higher ranges had a lower power/frequency. Based on these findings, it can be concluded that the vibration device can potentially be effective in dissolving phlegm in the lungs. The result is shown in Fig. 13.

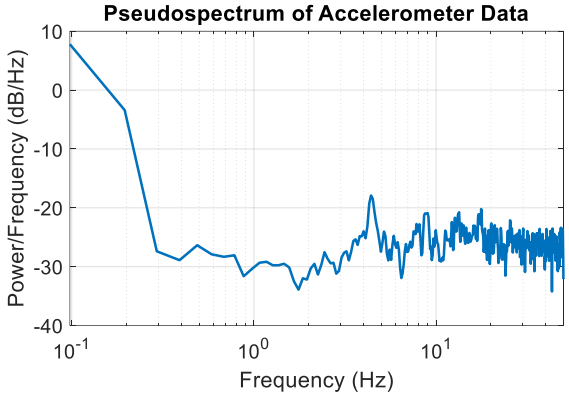

Fig. 13. Pseudospectrum of accelerometer profile

B. Second Result

The results of four different control systems, P, PI, PD, and PID, were obtained and presented in Fig. 14, Fig. 15, Fig. 16, and Fig. 17. The first graph in Figure shows the acceleration values in the x, y, and z axes. The second graph in figure shows the system control results using the g_{avg} signal as the output of the vibration device system. This graph includes the original value of g_{sum} to demonstrate the importance of the filter system. The third graph in figure shows the %duty cycle values of PWM delivered to the motor drive board for each of the control systems.

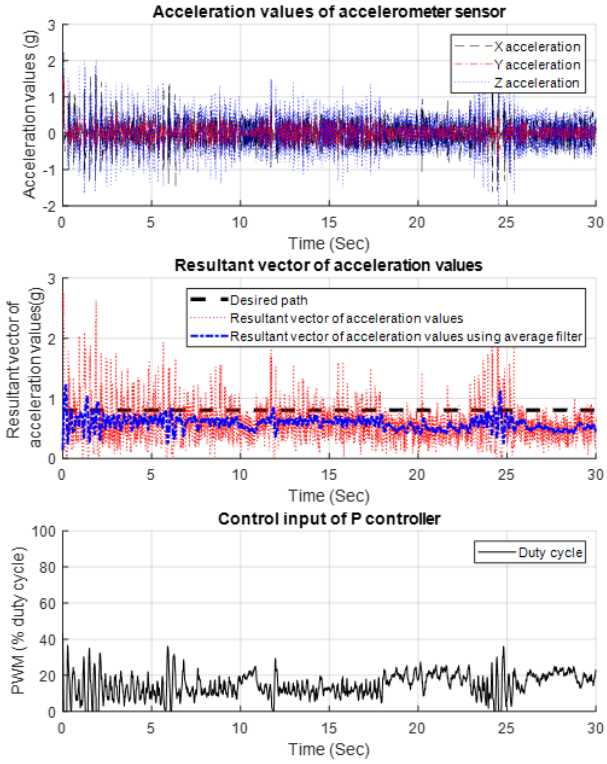

Fig. 14. The results of P controller

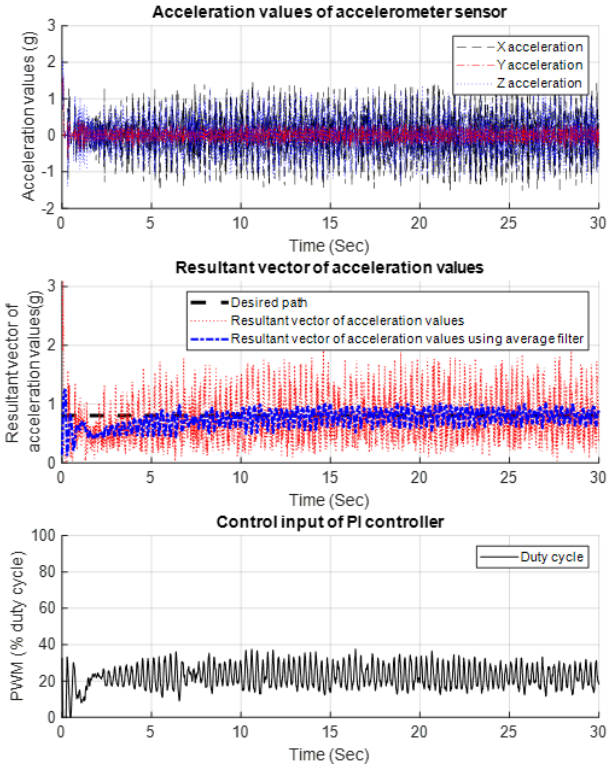

Fig. 15. The results of PI controller

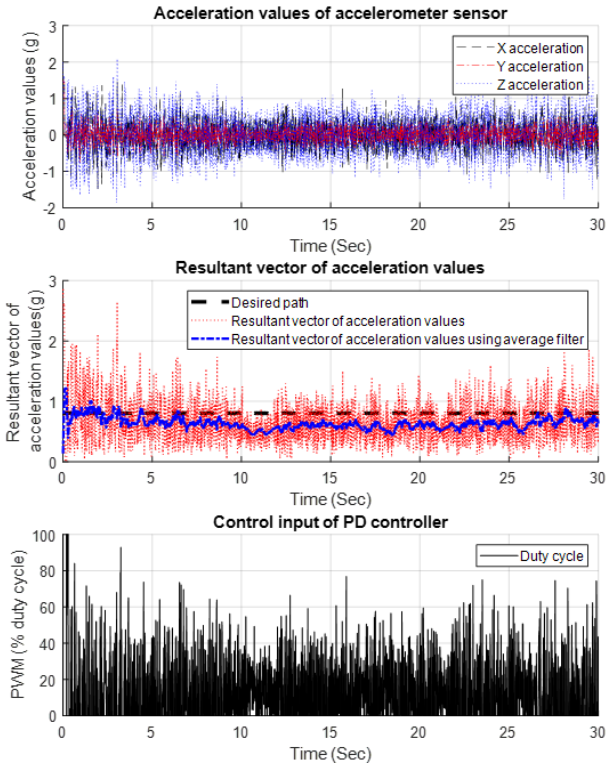

Fig. 16. The results of PD controller

During system testing, y_d was set at 0.8. The results indicated that the PID control system had the best performance, despite having a %OS value of 12% or a fluctuation of ±0.1 g when reaching a stable point. The PI control system had the second best efficiency with a %OS value of 25% or a fluctuation of ±0.2 g when reaching a stable point.

The PD control system had the third best efficiency with a %OS value of 12% or a fluctuation of ±0.1 g, but an offset value of 0.6, which was lower than the y_d value to be controlled when reaching a stable point. The P control system had the fourth best efficiency with a %OS value of 25% or a fluctuation of ±0.2 g, but with an offset value of 0.6, which was lower than the y_d value to be controlled when reaching a stable point. In general, the vibration device system requires an I term for processing to reach the setpoint and a D term for reducing the %OS within the system. This theory makes the PID system suitable for controlling the vibration device system. In the dataset of the resultant vector of acceleration values, a comparison will be made between the data obtained with the use of an average filter and the data obtained without it. The utilization of the average filter is essential in this control system as it aids in the precise control of the non-invasive pulmonary vibration device's vibrations, as demonstrated in Fig. 14 to Fig. 17.

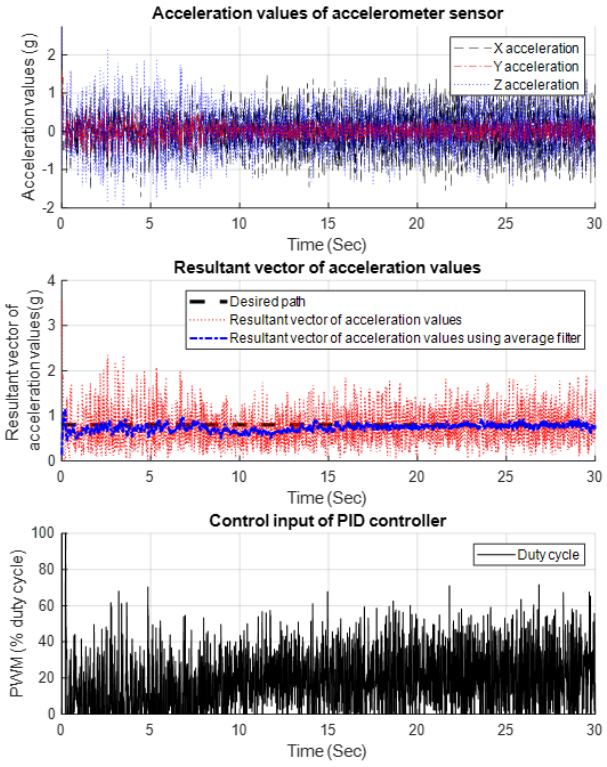

Fig. 17. The results of PID controller

C. *Third Result*

The third finding from healthcare research [84], [85] was based on the analysis of IRB documents (COA: 009/2021 and Protocol No: EC 20107-19) that were obtained to conduct the study. The details of the information obtained are as follows:

The data collection process in this research involved two main parts. The first part was related to the research tools used, which included the following:

Pulmonary vibration devices: This is an electrical device that helps remove phlegm from the upper respiratory tract through vibration with a frequency of 0-22 Hz. The voltage can be adjusted using a microcontroller to suit the patient's body weight. This device has been tested for safety and effectiveness in the laboratory by the Center for Biomedical

Engineering Innovation and Service at Rangsit University. It also has medical device certification according to the IEC 60601-1 series.

Pediatric pulse oximeter, this external device measures the level of oxygen saturation in the arteries (SpO2) at the fingertips, back of the hand, or instep. It has been checked by the manufacturer and staff with expertise in medical equipment from the College of Biomedical Sciences at Rangsit University.

Stethoscope, this tool is used to listen to breathing sounds before and after sputum drainage. Sterile sputum trap, this tool is used to assess the amount of sputum obtained after phlegm drainage and suction in pediatric pneumonia patients. The sputum was recorded in milliliters.

The second part of the data collection process involved an evaluation form to assess the effectiveness of sputum drainage. The form was developed from a review of relevant literature [12], [15], [77]-[79] and consisted of two main sections.

First, personal information of the pediatric patient: This included 9 items, such as age, gender, date of birth, date of admission to the hospital, diagnosis, signs and symptoms of pneumonia, first vital signs, past medical conditions or illnesses, and number of pneumococcal illnesses.

Second, efficacy evaluation forms for sputum drainage: This form consists of two parts. The first part was a clinical symptoms assessment form that was used to evaluate the clinical symptoms of pediatric patients with pneumonia before and after sputum suction, including respiratory rate, pulse rate, arterial oxygen saturation (SpO2) at the fingertips, and abnormal breathing sound locations. The second part was used to record the amount and nature of sputum obtained during the drainage process.

The quality of the research tools used in this study was assessed through a process of content validation. The tools used to collect data were brought to a panel of 5 experts, including 1 pediatrician specializing in pediatric critical care, 2 pediatric nurses specializing in respiratory and pediatric critical care, and 2 pediatric nurses and a physiotherapist with experience in caring for pediatric respiratory diseases and critically ill children. These experts examined the content of the tools to ensure their validity.

The content validity index (CVI) for the drainage efficacy questionnaire was 0.98, indicating a high level of content validity. Additionally, the human Cronbach's alpha coefficient was 0.87, indicating a high level of internal consistency. These results suggest that the research tools used in this study were of high quality and could be relied upon to collect accurate and reliable data. To collect information from hospitals and patients, the following process was followed:

First, a request for permission was sent to the hospital director, ward doctor, and head of the pediatric ward to introduce the researcher and clarify the purpose of the research, research process, and protection of the rights of the sample.

Research tools were prepared, and researchers and data collection assistants, including professional nurses and physical therapists with at least 2 years of experience in caring for pediatric patients with respiratory diseases, were trained on the objectives of the research and how to use the data collection tools. The intraconsistent confidence measure between the researcher and the research assistant, who is a registered nurse in the pediatric ward and has experience in caring for patients with pneumonia for more than 5 years (inter-rater reliability: IRR), was found to be 0.92.

Data collection in the control group was managed by assessing the clinical symptoms according to the efficacy evaluation form, providing basic information before conducting the research, and ensuring the safety of the sample. Sputum was drained using normal chest physical therapy, tapping and vibrating the lungs with the hands for 10 minutes before the meal to prevent suffocation. After suctioning, the amount of sputum was recorded, and the effectiveness of sputum drainage was evaluated after 2 minutes and 5 minutes of suctioning. Data were collected individually until 25 patients were completed, following which data collection was started in the experimental group.

Data collection in the experimental group. The researcher and the research assistant first evaluated the clinical symptoms using an efficacy assessment form for sputum drainage, and provided basic information on the research and safety precautions to the patients. Next, they used a pulmonary vibration device (as shown in Fig. 2) to perform sputum drainage. The device's acceleration values were adjusted based on the patient's weight, using values of 50-65% for patients weighing less than 10 kg (as shown in Fig. 18), and 65-85% for patients weighing more than 10 kg (as shown in Fig. 19). The device was used in intermittent mode for 10 minutes before the meal to prevent suffocation. After this, suction was performed and the amount of sputum was recorded. The effectiveness of sputum drainage was then evaluated after 2 and 5 minutes of suction, respectively. Data were collected for 25 cases individually, while ensuring that the rights of patients were protected, and their parents had provided written consent for the procedure.

The research findings in the healthcare field can be divided into two parts. The first part pertains to the individual characteristics of the participants. The control group included 25 individuals aged between 1 to 5 years and 11 months, with an average age of 2.25 years (SD=1.43). Among these individuals, 60% were males and 40% were females. The majority of them had interstitial pneumonia, out of which 44% had no co-morbidity, 88% had no underlying disease, and 96% had never been treated for pneumonia. In the past year, 80% of the individuals experienced inflammation. The experimental group, on the other hand, consisted of 25 participants aged between 1 to 3 years and 11 months, with an average age of 2.14 years (SD=1.13). Among these individuals, 56% were females and 44% were males. Out of these, 40% had interstitial pneumonia, 72% had no underlying disease, and 100% had not received any treatment for pneumonia in the previous year. Moreover, 48% of these individuals experienced inflammation.

The second part of the research findings pertains to the efficacy of expectorant drainage between the control group and the experimental group. After 2 minutes of sputum drainage, no significant differences were observed in various aspects, including respiratory rate, pulse rate, the level of oxygen saturation in the arteries of the fingertips, breathing sounds, and position. Similarly, after 5 minutes of sputum drainage, no significant differences were observed in breathing rate, pulse rate, the level of oxygen saturation in the arteries of the fingertips, and abnormal breathing sounds. No difference was found in these aspects (p=0.302).

Fig. 18. Patients weighing less than 10 kg

Fig. 19. Patients weighing more than 10 kg

After conducting a study on the effectiveness of chest physiotherapy in pediatric patients with pneumonia, it was found that the use of a pulmonary vibration device can promote sputum drainage similar to normal chest physiotherapy [15]. The study showed that there was no difference in the effectiveness of sputum drainage between the control group and the experimental group, but there were differences in various aspects such as respiration rate, pulse rate, oxygen saturation level, and abnormal breathing sound position [15].

It was observed that chest physiotherapy using a pulmonary vibration device and normal chest physiotherapy using hand tapping and vibration can cause vibration in the chest wall, which increases the pressure in the pleural space and increases the exhalation flow rate, resulting in easy elimination of packed sputum from the trachea [77], [80]. However, regular chest physiotherapy may cause unstable vibrations and fatigue and may not be performed continuously for the required 10-20 minutes [12], [15], [77]. On the other hand, the use of a pulmonary vibration device has a preset vibration frequency and acceleration value determined according to the patient's body weight, and there is a periodic vibration (intermittent mode) to prevent complications from continuous vibration [15].

The study also found that the use of a pulmonary vibration device is easy to use, convenient, and can be used by parents of pediatric pneumonia patients to care for them on the bed, thus reducing the fear of the procedure [15]. Additionally, the device can prevent the occurrence of airway obstruction, reduce respiratory resistance, improve the breathing process, and gas exchange of the patient, which ultimately results in a decrease in the patient's breathing rate [12], [80], [83].

Therefore, the use of a pulmonary vibration device can increase the efficiency of better phlegm drainage in pediatric pneumonia patients, making it a potential application for their care [15]. However, further studies are required to evaluate the satisfaction and complications associated with the use of the device [15].

D. Overall Results

The comprehensive findings of this study can be summarized. In experimental result 1, the initial experiment focused on evaluating the vibration device's frequency range using a PID controller. The outcomes revealed that the device operated within a frequency range below 20 Hz, demonstrating significant power/frequency characteristics. This suggests its potential effectiveness in addressing pulmonary congestion.

In experimental result 2, the second phase of experimentation aimed to assess the efficiency of various control systems (P, PI, PD, and PID) in managing the non-invasive pulmonary vibration device. The findings prominently favored the PID control system, as it exhibited the highest level of efficiency, making it the most suitable choice for device control.

In experimental result 3, the study transitioned to practical applications in pediatric patients. The results underscored that the non-invasive pulmonary vibration device, meticulously designed and tested based on established principles, could be effectively employed in real-world scenarios. This device boasts user friendliness, convenience, and the ability to minimize patient discomfort, rendering it a asset for pediatric care.

In summary, this research underscores the potential of the non-invasive pulmonary vibration device in assisting pediatric patients, particularly those grappling with pulmonary ailments. The device's performance, combined with the efficiency of the PID control system, hints at its feasibility as an alternative to traditional treatment approaches. Subsequent investigations should delve into patient satisfaction and potential complications associated with its implementation.

VI. CONCLUSION

In conclusion, this study has presented the design and development of a pulmonary vibration device aimed at facilitating secretion drainage in pediatric patients with

pneumonia. The utilization of an Arduino Uno board to control the vibration motor via accelerometer data has resulted in a promising solution for enhancing chest physiotherapy in the healthcare domain. The choice of the PID control system, guided by the Ziegler Nichols tuning technique, has been identified as the most suitable design for effectively controlling the device. This strategic decision underscores the potential for future research avenues, including investigations into PID controller gain adjustments and the exploration of alternative control strategies. While our comparative analysis with traditional hand tapping did not reveal significant differences, the pulmonary vibration device's potential in aiding sputum drainage and chest physiotherapy for pediatric pneumonia patients remains evident. Furthermore, its applicability could extend beyond this specific patient group, benefiting diverse populations, including elderly individuals requiring similar treatments. This study underscores the evolving landscape of healthcare, where technology plays a pivotal role in advancing patient care. The horizon for further research in this interdisciplinary field is expansive, encompassing the refinement of control mechanisms and the exploration of broader applications. By merging technology and healthcare, this study illuminates a promising path for future investigations into healthcare innovation.

ACKNOWLEDGMENT

The completion of this research project would not have been possible without the support and assistance of several individuals and organizations, to whom the researcher is sincerely grateful. First and foremost, the researchers would like to express their gratitude to the director and staff of both Maechan Hospital and Maesai Hospital, located in Chiang Rai Province, Thailand, for their invaluable assistance in collecting data and facilitating the research process. The researchers would like to extend special thanks to the research assistants who played a vital role in the project, including Wannapat Vongleasagoon, pediatrician at Maechan hospital; Sopa Kaewrakmook, a registered nurse at Maechan hospital; Jiriyarat Nitipipatkosol, pediatrician at Maesai hospital; and Satreerus Thakhamma, registered nurse at Maesai hospital. Their dedication and hard work in collecting and organizing data were critical to the success of the study. The researcher would also like to thank the sample group and all participating families for their willingness to provide valuable information and make this study possible. Furthermore, the researcher would like to acknowledge Mae Fah Luang University for providing the necessary resources and funding to carry out this research, including issuing the IRB documents (COA: 009/2021 and Protocol No: EC 20107-19). Finally, the researcher expresses their gratitude to the research institute, academic services center, and College of Biomedical Engineering at Rangsit University for their generous grant of research funding to the research team and medical device certification according to the IEC 60601-1 series. Once again, the researcher would like to thank everyone who contributed to this study and made it possible.

REFERENCES

[1] P. T. Nguyen, H. T. Tran, D. A. Fitzgerald, T. S. Tran, S. M. Graham, and B. J. Marais, "Characterisation of children hospitalised with pneumonia in central Vietnam: a prospective study," *European Respiratory Journal*, vol. 54, no. 1, 2019. doi: 10.1183/13993003.02256-2018.

[2] K. Kumthip, P. Khamrin, H. Ushijima, and N. Maneekarn, "Enteric and non-enteric adenoviruses associated with acute gastroenteritis in pediatric patients in Thailand, 2011 to 2017," *PloS one*, vol. 14, no. 8, pp. 1–12, 2019, doi: 10.1371/journal.pone.0220263.

[3] C. S. Mani, "Acute pneumonia and its complications," in *Principles and Practice of Pediatric Infectious Diseases*, vol. 238, 2018. doi:https: 10.1016/B978-0-323-40181-4.00034-7.

[4] X. X. Ao, "The epidemiology of hospital death following pediatric severe community acquired pneumonia," *Italian Journal of Pediatrics*, vol. 47, no. 1, pp. 1-5, 2021. doi: 10.1186/s13052-021-00966-0.

[5] T. Jaikarn and N. Wongcharoen, "Incidence Rates and Impact of Pneumonia in Pong Hospital," *Journal of Royal Thai Army Nurses*, vol. 22, no. 1, pp. 351-360, Apr. 2021.

[6] D. A. McAllister *et al*., "Global, regional, and national estimates of pneumonia morbidity and mortality in children younger than 5 years between 2000 and 2015: a systematic analysis," *Lancet Glob Health*, vol. 7, no. 1, pp. e47-57, 2019. doi: 10.1016/S2214-109X(18)30408-X.

[7] P. Klangka, "A Development of Discharge Planning Model for Pediatric Patients with Pneumonia Using Family and Caregiver Participation," *Journal of Vongchavalitkul University*, vol. 32, no. 2, pp. 40-49, 2019.

[8] R. T. Ellison III and G. R. Donowitz, "Acute pneumonia," in *Mandell, Douglas, and Bennett's Principles and Practice of Infectious Diseases*, pp. 823, 2015, doi: 10.1016/B978-1-4557-4801-3.00069-2.

[9] A. Tulebayeva, M. Sharipova, and R. Boranbayeva, "Respiratory dysfunction in children and adolescents with mucopolysaccharidosis types I, II, IVA, and VI," *Diagnostics*, vol. 10, no. 2, p. 63, 2020, doi: 10.3390/diagnostics10020063.

[10] A. O. Odeyemi, A. O. Oyedeji, O. J. Adebami, and E. Agelebe, "Complications of pneumonia and its associated factors in a pediatric population in Osogbo, Nigeria," *Nigerian Journal of Paediatrics*, vol. 47, no. 4, pp. 318-323, 2020, doi: 10.4314/njp.v47i4.4.

[11] D. P. Pozuelo-Carrascosa, A. Torres-Costoso, C. Alvarez-Bueno, I. Cavero-Redondo, P. L. Muñoz, and V. Martinez-Vizcaino, "Multimodality respiratory physiotherapy reduces mortality but may not prevent ventilator-associated pneumonia or reduce length of stay in the intensive care unit: a systematic review," *Journal of physiotherapy*, vol. 64, no. 4, pp. 222-228, 2018.

[12] G. S. Chaves, D. A. Freitas, T. A. Santino, P. A. M. Nogueira, G. A. Fregonezi, and K. M. Mendonca, "Chest physiotherapy for pneumonia in children," *Cochrane Database of Systematic Reviews*, no. 1, 2019.

[13] A. Spinou and J. D. Chalmers, "Using airway clearance techniques in bronchiectasis: Halfway there," *Chest*, vol. 158, no. 4, pp. 1298-1300, 2020, doi: 10.1016/j.chest.2020.07.062.

[14] G. Leemans, D. Belmans, C. Van Holsbeke, B. Becker, D. Vissers, K. Ides, S. Verhulst, and K. Van Hoorenbeeck, "The effectiveness of a mobile high-frequency chest wall oscillation (HFCWO) device for airway clearance," *Pediatric Pulmonology*, vol. 55, no. 8, pp. 1984-1992, 2020, doi: 10.1002/ppul.24784.

[15] W. K. Abdelbasset and T. Elnegamy, "Effect of chest physical therapy on pediatrics hospitalized with pneumonia," *International Journal of Health and Rehabilitation Science*, vol. 4, no. 4, pp. 219-226, 2015, doi: 10.5455/ijhrs.000000095.

[16] C. Gibson, F. Eubanks, and F. Hobson, "A Systems Approach to Medical-Device Compliance with IEC 60601-1: 2005," *INCOSE International Symposium*, vol. 15, no. 4, pp. 39-45, 2012, doi: 10.1002/inst.201215439.

[17] J. Susilo, A. Febriani, U. Rahmalisa, and Y. Irawan, "Car parking distance controller using ultrasonic sensors based on Arduino Uno," *Journal of Robotics and Control (JRC)*, vol. 2, no. 5, pp. 353-356, 2021, doi: 10.18196/jrc.25106.

[18] E. S. Rahayu, A. Ma'arif, and A. Çakan, "Particle swarm optimization (PSO) tuning of PID control on DC motor," *International Journal of Robotics and Control Systems*, vol. 2, no. 2, pp. 435-447, 2022, doi: 10.31763/ijrcs.v2i2.476.

[19] E. W. Suseno and A. Ma'arif, "Tuning of PID controller parameters with genetic algorithm method on DC motor," *International Journal of Robotics and Control Systems*, vol. 1, no. 1, pp. 41-53, 2021, doi: 10.31763/ijrcs.v1i1.249.

[20] D. S. Febriyan and R. D. Puriyanto, "Implementation of DC motor PID control on conveyor for separating potato seeds by weight,"

International Journal of Robotics and Control Systems, vol. 1, no. 1, pp. 15-26, 2021, doi: 10.31763/ijrcs.v1i1.221.

[21] P. Chotikunnan and R. Chotikunnan, "Dual design PID controller for robotic manipulator application," *Journal of Robotics and Control (JRC)*, vol. 4, no. 1, pp. 23-34, 2023, doi: 10.18196/jrc.v4i1.16990.

[22] E. S. Ghith and F. A. A. Tolba, "Design and optimization of PID controller using various algorithms for micro-robotics system," *Journal of Robotics and Control (JRC)*, vol. 3, no. 3, pp. 244-256, 2022, doi: 10.18196/jrc.v3i3.14827.

[23] A. K. Hado, B. S. Bashar, M. M. A. Zahra, R. Alayi, Y. Ebazadeh, and I. Suwarno, "Investigating and optimizing the operation of microgrids with intelligent algorithms," *Journal of Robotics and Control (JRC)*, vol. 3, no. 3, pp. 279-288, 2022, doi: 10.18196/jrc.v3i3.14772.

[24] E. H. Kadhim and A. T. Abdulsadda, "Mini drone linear and nonlinear controller system design and analyzing," *Journal of Robotics and Control (JRC)*, vol. 3, no. 2, pp. 212-218, 2022, doi: 10.18196/jrc.v3i2.14180.

[25] J. An, F. You, M. Wu, and J. She, "Iterative learning control for nonlinear weighing and feeding process," *Mathematical Problems in Engineering*, vol. 2018, 2018, doi: 10. 1155/2018/9425902.

[26] X. Li, J. Liu, L. Wang, K. Wang, and Y. Li, "Welding process tracking control based on multiple model iterative learning control," *Mathematical Problems in Engineering*, vol. 2019, 2019, doi: 10.1155/2019/6137352.

[27] M. A. Hadj-Abdelkader, G. Bourhis, and B. Cherki, "Haptic feedback control of a smart wheelchair," *Applied Bionics and Biomechanics*, vol. 9, no. 2, pp. 181-192, 2012, doi: 10.3233/ABB-2012-0067.

[28] K. Sukerkar, D. Suratwala, A. Saravade, J. Patil, and R. D'britto, "Smart wheelchair: a literature review," *Mental Retardation*, vol. 5, no. 5. 4, pp. 5-6, 2018, doi: 10.11591/ijict.v7i2.pp63-66.

[29] D. Kumar, R. Malhotra, and S. R. Sharma, "Design and construction of a smart wheelchair," *Procedia Computer Science*, vol. 172, pp. 302-307, 2020, doi: https: 10.1016/j.procs.2020.05.048.

[30] K. Rahimunnisa, M. Atchaiya, B. Arunachalam, and V. Divyaa, "AI-based smart and intelligent wheelchair," *Journal of Applied Research and Technology*, vol. 18, no. 6, pp. 362-367, 2020, doi: 10.22201/icat.24486736e.2020.18.6.1351.

[31] A. Sharmila, A. Saini, S. Choudhary, T. Yuvaraja, and S. G. Rahul, "Solar Powered Multi-Controlled Smart Wheelchair for Disabled: Development and Features," *Journal of Computational and Theoretical Nanoscience*, vol. 16, no. 11, pp. 4889-4900, 2019.

[32] M. A. Awais, M. Z. Yusoff, N. Yahya, S. Z. Ahmed, and M. U. Qamar, "Brain controlled wheelchair: a smart prototype," in *Journal of Physics: Conference Series*, vol. 1529, no. 4, p. 042075, April 2020, doi: 10.1088/1742-6596/1529/4/042075.

[33] M. R. Islam, M. R. T. Hossain, and S. C. Banik, "Synchronizing of stabilizing platform mounted on a two-wheeled robot," *Journal of Robotics and Control (JRC)*, vol. 2, no. 6, pp. 552-558, 2021, doi: 10.18196/jrc.26136.

[34] F. A. Raheem, B. F. Midhat, and H. S. Mohammed, "PID and fuzzy logic controller design for balancing robot stabilization," *Iraqi Journal of Computers, Communications, Control and Systems Engineering*, vol. 18, no. 1, pp. 1-10, 2018, doi: 10.33103/uot.ijccce.18.1.1.

[35] C. Iwendi, M. A. Alqarni, J. H. Anajemba, A. S. Alfakeeh, Z. Zhang, and A. K. Bashir, "Robust navigational control of a two-wheeled self-balancing robot in a sensed environment," *IEEE Access*, vol. 7, pp. 82337-82348, 2019, doi: 10.1109/ACCESS.2019.2923916.

[36] I. Gandarilla, V. Santibañez, and J. Sandoval, "Control of a self-balancing robot with two degrees of freedom via IDA-PBC," *ISA Transactions*, vol. 88, pp. 102-112, 2019, doi: 10.1016/j.isatra.2018.12.014.

[37] Y. Su, T. Wang, K. Zhang, C. Yao, and Z. Wang, "Adaptive nonlinear control algorithm for a self-balancing robot," *IEEE Access*, vol. 8, pp. 3751-3760, 2019, doi: 10.1109/ACCESS.2019.2963110.

[38] F. Jiménez, I. Ruge, and A. Jiménez, "Modeling and Control of a Two Wheeled Self-Balancing Robot: a didactic platform for control engineering education," *LACCEI Inc*., 2020, doi: 10.18687/LACCEI2020.1.1.556.

[39] T. Terakawa, M. Komori, K. Matsuda, and S. Mikami, "A Novel Omnidirectional Mobile Robot With Wheels Connected by Passive Sliding Joints," *IEEE/ASME Trans. Mechatronics*, vol. 23, no. 4, pp. 1716–1727, Aug. 2018, doi: 10.1109/TMECH.2018.2842259.

[40] M. A. Al Mamun, M. T. Nasir, and A. Khayyat, "Embedded System for Motion Control of an Omnidirectional Mobile Robot," *IEEE Access*, vol. 6, no. 8, pp. 86722–6739, 2018, doi: 10.1109/ACCESS.2018.2794441.

[41] P. Shen, X. Zhang, and Y. Fang, "Complete and Time-Optimal PathConstrained Trajectory Planning With Torque and Velocity Constraints: Theory and Applications," *IEEE/ASME Trans. Mechatronics*, vol. 23, no. 2, pp. 735–746, Apr. 2018, doi: 10.1109/TMECH.2018.2810828.

[42] B. A. Gebre and K. V. Pochiraju, "Machine Learning Aided Design and Analysis of a Novel Magnetically Coupled Ball Drive," *IEEE/ASME Trans. Mechatronics*, vol. 24, no. 5, pp. 1942–1953, Oct. 2019, doi: 10.1109/TMECH.2019.2929956.

[43] M. Ferro, A. Paolillo, A. Cherubini, and M. Vendittelli, "VisionBased Navigation of Omnidirectional Mobile Robots," *IEEE Robot. Autom. Lett.*, vol. 4, no. 3, pp. 2691–2698, Jul. 2019, doi: 10.1109/LRA.2019.2913077.

[44] A. Dhyani, M. K. Panda, and B. Jha, "Moth-flame optimization-based fuzzy-PID controller for optimal control of active magnetic bearing system," *Iranian Journal of Science and Technology, Transactions of Electrical Engineering*, vol. 42, no. 4, pp. 451-463, 2018, doi: 10.1007/s40998-018-0077-1.

[45] H. Maghfiroh, A. Ramelan, and F. Adriyanto, "Fuzzy-PID in BLDC motor speed control using MATLAB/Simulink," *Journal of Robotics and Control (JRC)*, vol. 3, no. 1, pp. 8-13, 2022, doi: 10.18196/jrc.v3i1.10964.

[46] S. Gobinath and M. Madheswaran, "Deep Perceptron Neural Network with Fuzzy PID Controller for Speed Control and Stability Analysis of BLDC Motor," *Soft Computing*, vol. 24, no. 13, pp. 10161-10180, 2020, doi: 10.1007/s00500-019-04532-z.

[47] K. Vanchinathan and N. Selvaganesan, "Adaptive Fractional Order PID Controller Tuning for Brushless DC Motor Using Artificial Bee Colony Algorithm," *Results in Control and Optimization*, vol. 4, 2021, doi: 10.1016/j.rico.2021.100032.

[48] P. Dutta and S. K. Nayak, "Grey Wolf Optimizer Based PID Controller for Speed Control of BLDC Motor," *Journal of Electrical Engineering & Technology*, vol. 16, no. 2, pp. 955-961, 2021, doi: 10.1007/s42835-021-00660-5.

[49] A. Ma'arif and A. Çakan, "Simulation and arduino hardware implementation of dc motor control using sliding mode controller," *Journal of Robotics and Control (JRC)*, vol. 2, no. 6, pp. 582, doi: 10.18196/jrc.26140.

[50] A. Latif, A. Z. Arfianto, H. A. Widodo, R. Rahim, and E. T. Helmy, "Motor DC PID System Regulator for Mini Conveyor Drive Based on MATLAB," *Journal of Robotics and Control (JRC)*, vol. 1, no. 6, pp. 185-190, 2020, doi: 10.18196/jrc.1636.

[51] B. Hekimoğlu, "Optimal Tuning of Fractional Order PID Controller for DC Motor Speed Control via Chaotic Atom Search Optimization Algorithm," *IEEE Access*, vol. 7, pp. 38100-38114, 2019, doi: 10.1109/ACCESS.2019.2905961.

[52] A. Ma'arif and N. R. Setiawan, "Control of DC motor using integral state feedback and comparison with PID: simulation and Arduino implementation," *Journal of Robotics and Control (JRC)*, vol. 2, no. 5, pp. 456-461, 2021, doi: 10.18196/jrc.25122.

[53] S. K. Mallempati, G. Satheesh, and S. Peddakotla, "Design of optimal PI controller for torque ripple minimization of SVPWM-DTC of BLDC motor," *International Journal of Power Electronics and Drive Systems*, vol. 14, no. 1, p. 283, 2023, doi: https://doi.org/10.11591/ijpeds.v14.i1.

[54] Y. Li, K. H. Ang, and G. C. Chong, "PID control system analysis and design," *IEEE Control Systems Magazine*, vol. 26, no. 1, pp. 32-41, 2006, doi: 10. 1109/MCS. 2006. 1580152.

[55] C. T. Chao, N. Sutarna, J. S. Chiou, and C. J. Wang, "An optimal fuzzy PID controller design based on conventional PID control and nonlinear factors," *Applied Sciences*, vol. 9, no. 6, p. 1224, 2019, doi: 10.3390/app9061224.

[56] R. P. Borase, D. K. Maghade, S. Y. Sondkar, and S. N. Pawar, "A review of PID control, tuning methods and applications," *International Journal of Dynamics and Control*, vol. 9, no. 2, pp. 818-827, 2021, doi: 10.1007/s40435-020-00665-4.

[57] S. J. Hammoodi, K. S. Flayyih, and A. R. Hamad, "Design and Implementation of Speed Control System for DC Motor Based on PID Control and Matlab Simulink," *International Journal of Power*

Electronics and Drive Systems, vol. 11, no. 1, p. 127, 2020, doi: 10.11591/ijpeds.v11.i1.

[58] D. Somwanshi, M. Bundele, G. Kumar, and G. Parashar, "Comparison of Fuzzy-PID and PID Controller for Speed Control of DC Motor Using LabVIEW," in *Procedia Computer Science*, vol. 152, pp. 252-260, 2019, doi: 10.1016/j.procs.2019.05.019.

[59] V. V. Patel, "Ziegler-Nichols Tuning Method," *Resonance*, vol. 25, no. 10, pp. 1385-1397, 2020, doi: 10.1007/s12045-020-1058-z.

[60] T. Y. Wu, Y. Z. Jiang, Y. Z. Su, and W. C. Yeh, "Using Simplified Swarm Optimization on Multiloop Fuzzy PID Controller Tuning Design for Flow and Temperature Control System," *Applied Sciences*, vol. 10, no. 23, p. 8472, 2020, doi: 10.3390/app10238472.

[61] R. R. Alla, N. Lekyasri, and K. Rajani, "PID Control Design for Second Order Systems," *Int. J. Eng. Manuf.*, vol. 9, no. 4, pp. 45-56, 2019, doi: 10.5815/ijem.2019.04.04.

[62] E. Bashier and O. Mohammed, "Optimally Tuned Proportional Integral Derivatives (PID) Controllers for Set-Point," *Journal of Engineering and Computer Science (JECS)*, vol. 13, no. 1, pp. 48-53, 2019.

[63] C. Dalen and D. Di Ruscio, "Performance optimal PI controller tuning based on integrating plus time delay models," *Algorithms*, vol. 11, no. 6, pp. 86, 2018, doi: 10.3390/a11060086.

[64] S. Kai-bo, H. Jian, and L. Lin-tao, "A New Method of DC Motor Speed Regulation based on STM32," *Journal of Astronautic Metrology and Measurement*, vol. 38, no. 2, p. 87, 2018, doi: 10.12060/j.issn.1000-7202.2018.02.18.

[65] S. Jain and Y. V. Hote, "Design of FOPID Controller Using BBBC via ZN Tuning Approach: Simulation and Experimental Validation," *IETE Journal of Research*, vol. 68, no. 5, pp. 3356-3370, 2022, doi: 10.1080/03772063.2020.1756937.

[66] V. Dubey, "Comparative Analysis of PID Tuning Techniques for Blood Glucose Level of Diabetic Patient," *Turkish Journal of Computer and Mathematics Education (TURCOMAT)*, vol. 12, no. 11, pp. 2948-2953, 2021.

[67] A. O. Amole, O. E. Olabode, D. O. Akinyele, and S. G. Akinjobi, "Optimal Temperature Control Scheme for Milk Pasteurization Process Using Different Tuning Techniques for a Proportional Integral Derivative Controller," *Iranian Journal of Electrical and Electronic Engineering*, vol. 2170, pp. 2170-2170, 2022, doi: 10.22068/IJEEE.18.3.2170.

[68] N. A. Rao and C. R. Kumar, "Speed Control of Brushless Dc Motor by Using PID and Fuzzy Logic Controller," *International Journal of Innovative Research in Technology*, vol. 4, no. 6, 2019.

[69] P. Saini and C. Sharma, "Comparative Analysis of Controller Tuning Techniques for Dead Time Processes," *International Journal of Mathematical, Engineering and Management Sciences*, vol. 4, no. 3, pp. 803, 2019, doi: 10.33889/IJMEMS.2019.4.3-063.

[70] E. Kesavan, K. M. Junaid, and B. Jaison, "Design and Analysis of Different Tuning Strategies of PI Controller for Distillation Column," *International Journal of Control Systems and Robotics*, vol. 4, 2019.

[71] Z. Qi, Q. Shi, and H. Zhang, "Tuning of Digital PID Controllers Using Particle Swarm Optimization Algorithm for a CAN-Based DC Motor Subject to Stochastic Delays," *IEEE Transactions on Industrial Electronics*, vol. 67, no. 7, pp. 5637-5646, doi: 10.1109/TIE.2019.2934030.

[72] M. M. Nishat, F. Faisal, A. J. Evan, M. M. Rahaman, M. S. Sifat, and H. F. Rabbi, "Development of Genetic Algorithm (GA) Based Optimized PID Controller for Stability Analysis of DC-DC Buck Converter," *Journal of Power and Energy Engineering*, vol. 8, no. 9, p. 8, 2020, doi: 10.4236/jpee.2020.89002.

[73] H. Feng, C. B. Yin, W. W. Weng, W. Ma, J. J. Zhou, W. H. Jia, and Z. L. Zhang, "Robotic excavator trajectory control using an improved GA based PID controller," *Mechanical Systems and Signal Processing*, vol. 105, pp. 153-168, 2018, doi: 10.1016/j.ymssp.2017.12.014.

[74] S. Mahfoud, A. Derouich, N. El Ouanjli, M. El Mahfoud, and M. Taoussi, "A New Strategy-Based PID Controller Optimized by Genetic Algorithm for DTC of the Doubly Fed Induction Motor," *Systems*, vol. 9, no. 2, p. 37, 2021, doi: 10.3390/systems9020037.

[75] R. Cookson, M. Asaria, S. Ali, R. Shaw, T. Doran, and P. Goldblatt, "Health equity monitoring for healthcare quality assurance," *Social Science & Medicine*, vol. 198, pp. 148–156, 2018, doi: 10.1016/j.socscimed.2018.01.004.

[76] J. Cohen, "Statistical power analysis," in *Current Directions in Psychological Science*, vol. 1, no. 3, pp. 98-101, doi: 10.1111/1467-8721.ep10768783.

[77] H. A. Hussein and G. A. Elsamman, "Effect of chest physiotherapy on improving chest airways among infants with pneumonia," *Journal of American Science*, vol. 7, no. 9, pp. 460-466, 2011.

[78] F. Longhini, A. Bruni, E. Garofalo, C. Ronco, A. Gusmano, G. Cammarota, L. Pasin, P. Frigerio, D. Chiumello, and P. Navalesi, "Chest physiotherapy improves lung aeration in hypersecretive critically ill patients: a pilot randomized physiological study," *Crit Care*, vol. 24, no. 1, p. 479, 2020, doi:https://doi.org/10.1186/s13054-020-03198-6, doi: 10.1186/s13054-020-03198-6.

[79] S. Kluayhomthong, W. Khrisanapant, S. Chaisuksant, and C. U. Jones, "Effectiveness of a new breathing device 'BreatheMAX®' to increase air way secretion clearance in patients with ventilatory dependence," *Journal of Medical Technology and Physical Therapy*, vol. 23, no. 1, pp. 95-108, 2011.

[80] N. E. Lestari, N. Nurhaeni, and S. Chodidjah, "The combination of nebulization and chest physiotherapy improved respiratory status in children with pneumonia," *Enfermeria Clinica*, vol. 28, pp. 19-22, 2018, doi: 10.1016/S1130-8621(18)30029-9.

[81] L. Corten, J. Jelsma, A. Human, S. Rahim, and B. M. Morrow, "Assisted autogenic drainage in infants and young children hospitalized with uncomplicated pneumonia, a pilot study," *Physiotherapy Research International*, vol. 23, no. 1, p. e1690, 2018, doi: 10.1002/pri.1690.

[82] F. Van Ginderdeuren, Y. Vandenplas, M. Deneyer, S. Vanlaethem, R. Buyl, and E. Kerckhofs, "Effectiveness of airway clearance techniques in children hospitalized with acute bronchiolitis," *Pediatric Pulmonology*, vol. 52, no. 2, pp. 225-231, 2017, doi: 10.1002/ppul.23495.

[83] F. R. Pinto, A. S. Alexandrino, L. Correia-Costa, and I. Azevedo, "Ambulatory chest physiotherapy in mild-to-moderate acute bronchiolitis in children under two years of age—A randomized control trial," *Hong Kong Physiotherapy Journal*, vol. 41, no. 2, pp. 99-108, 2021.

[84] N. Seethikaew, P. Chotikunnan, and J. Supruang, "Innovation development vibrate for drainage secretion of pediatric patients," *Journal of The Royal Thai Army Nurses*, vol. 23, no. 2, pp. 418-427, 2022.

[85] N. Seethikaew, P. Chotikunnan, W. Vongleasagoon, J. Nitipipatkosol, S. Kaewrakmook, and S. Thakhamma, "Effects of using chest vibration innovation on the efficacy of secretion drainage in children with pneumonia," *Songklanagarind Journal of Nursing*, vol. 42, no. 1, pp. 85-96, 2022.